Singularity Theory Approach to Ideal Binary Distillation

Costin S. Bildea and Alexandre C. Dimian
Dept. of Chemical Engineering, University of Amsterdam, 1018 WV Amsterdam, The Netherlands

Distillation columns with ideal vapor–liquid equilibrium may display multiple steady states. Jacobsen and Skogestad (1991) pointed out the following sources of multiplicity: (1) the nonlinearity of the transformation between mass and molar flow rates; and (2) interaction between flows and composition due to energy balance. Kienle et al. (1995) found experimentally multiple steady states in the methanol–propanol separation, the first item above being the source of multiplicity. They computed the locus of limit points (codimension-1 singularities) and showed how the interaction with feasibility boundaries leads to different bifurcation diagrams. Similar results were obtained for the equilibrium model with constant molar overflow and for the detailed model, including energy balance and mass-transfer resistance. However, they considered only one column design and only one mixture. Moreover, they did not provide a complete classification of the steady-state behavior.

This work analyzes the multiplicity of states in binary distillation by rigorous application of the singularity theory (Balakotaiah and Luss, 1984; Golubitsky and Schaeffer, 1985). We consider the mass-reflux flow rate (L_w) as bifurcation parameter and compute codimension-2 varieties that divide the feed composition (z_F)–boilup (V) parameter space into regions where different types of bifurcation diagrams exist. Finally, we investigate the effect of physical and design parameters on the location and extent of the multiplicity regions.

State Multiplicity in Ideal, Binary Distillation

Steady-state multiplicity does exist in distillation. Let's consider the separation of a binary mixture with ideal vapor–liquid equilibrium and assume constant molar overflows. The reflux is specified on mass basis, while the boilup flow rate is specified on a molar basis (the L_w V configuration). The model equations are well known (Seader and Henley, 1998). We note that the tray molar balance equation can be written in dimensionless form by dividing by the feed flow rate ($\overline{F}$). For this reason, we will use the symbols L (molar reflux), V (molar boilup), D (distillate flow rate), B (bottom flow rate) for dimensionless variables, and the symbols $\overline{F}$, $\overline{L}$, $\overline{V}$, $\overline{D}$, $\overline{B}$ for dimensional variables composition notation refers to light component.

Two feasibility boundaries exist for distillation. At *total reflux*, the distillate flow rate is zero and only a bottom product is obtained (this is different from the total reflux used in the Fenske equation, which applies for a closed system). Similarly, at *total reboil*, there is no bottom product but a distillate.

Figure 1 explains the occurrence of state multiplicity. The solid line represents the dependence of distillate composition vs. molar reflux, obtained from tray-by-tray material balance and equilibrium equations. The dashed line represents the relationship between molar reflux and distillate composition, for fixed mass reflux. The two curves may intersect at three points, corresponding to three different steady states that are possible for the same operating parameters (mass reflux and boilup). The McCabe-Thiele diagrams of the three operating points are also displayed.

We remark that the middle steady state is unstable. Consider a small, positive deviation of the distillate composition. The molar reflux becomes higher than the one necessary to achieve the actual purity; hence, the distillate composition will increase further, until the upper operating point is reached.

Solution Method

The methodology we will use to classify the steady-state behavior may be applied to systems that are described by a single intrinsic variable. This implies that, at least theoretically, it is possible to reduce the model equations to one equation with one variable. To demonstrate the validity of this assumption, we outline one possible approach to the solution of model equations.

We start with an initial guess for the distillate composition, x_D. The dimensionless molar reflux is given by

$$L = \frac{L_w}{1 + (M_1/M_2 - 1)\cdot x_D}, \tag{1}$$

where M_1/M_2 is the molar weight ratio, $L_w = \overline{L}_w/(\overline{F}\cdot M_2)$ and $L = \overline{L}/\overline{F}$ are the dimensionless mass and molar reflux, respectively.

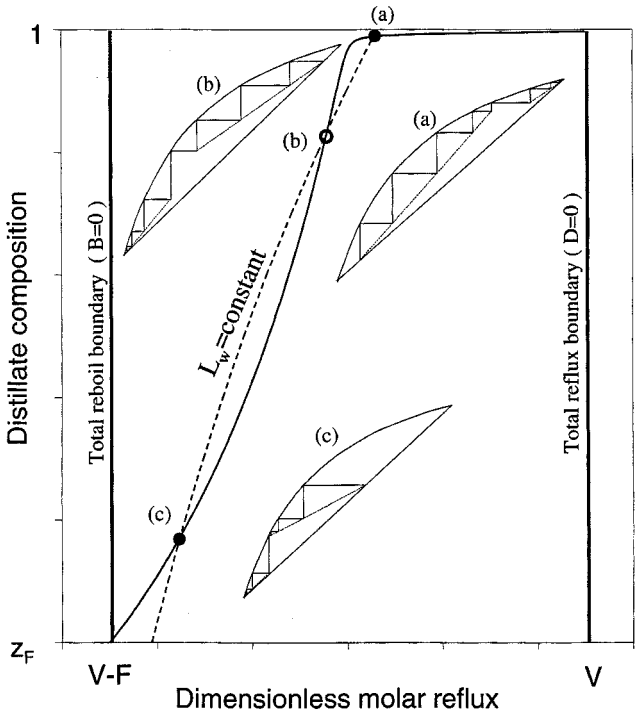

Figure 1. State multiplicity in ideal, binary distillation.

Continuous line represents distillate composition vs. molar reflux. Dashed line represents the relationship between molar reflux and distillate composition, for fixed mass reflux. There are three different feasible steady states. The middle state is unstable. $\alpha = 3.55$; $M_1 = 32$; $M_2 = 60$; $z_F = 0.5$; $V = 2$ kmol/kmol feed; $L_w = 50$ kg/kmol feed; $N = 8$; $N_F = 4$.

Application of the equilibrium and operating equations gives the composition of the bottom product:

$$\begin{aligned} &y_1 = x_D \\ &x_1 = e(y_1) \\ &\text{do} \quad k = 2 \ldots N \\ &y_k = o(x_{k-1}) \\ &x_k = e(y_k) \\ &\text{end do} \end{aligned} \tag{2}$$

where x_k and y_k are the composition of the liquid and vapor leaving the kth tray, and $e(.)$ and $o(.)$ represent equilibrium and operating equations, respectively.

Finally, the global mole balance is checked, and x_D is updated.

$$f(x_D) = F \cdot z_F - (V - L) \cdot x_D - (F - V + L) \cdot x_N = 0. \tag{3}$$

We remark that this approach is independent of the vapor–liquid equilibrium model used. Moreover, no fundamental limitations arise by including the energy balance. Although not straightforward, reduction to a one-equation model is theoretically possible.

Singularity theory states that the qualitative features of the bifurcation diagram may change only when the parameter set crosses the *hysteresis* (H), *isola*, or *double-limit* varieties. Only the hysteresis variety exists for ideal, constant molar overflow, binary distillation with mass reflux as bifurcation parameter. When the hysteresis variety is crossed, the number of possible steady states changes by two, as two limit points appear or disappear.

When feasibility boundaries exist, the bifurcation diagram may also change at special sets of parameters (Balakotaiah and Luss, 1984). In this work we considered:

- The *boundary-limit set:* a limit point exists at a feasibility boundary. There are two such sets, corresponding to one limit point at the total reboil (BL_1) or total reflux (BL_2) boundaries, respectively.
- The *cross-and-limit set:* the position of one limit point relative to one solution located at the feasibility boundary changes. There are two such sets, corresponding to total reboil (CL_1) or total reflux (CL_2) and one limit point occurring for the same value of the bifurcation parameter.
- The *double-cross set* (DC): the relative position of two solutions located at the feasibility boundary changes. There is one double-cross set, corresponding to total reboil and total reflux occurring for the same value of the bifurcation parameter.

The varieties just mentioned are 2-codimensional, that is, they fix the value of two parameters. Balakotaiah and Luss (1984) present their defining equations. The derivatives involved in the definition of the singular points can be easily computed by successively applying the chain rule for differentiation.

For the first stage,

$$\frac{\partial y_1}{\partial x_D} = 1. \tag{4}$$

x_1 is computed from y_1 using the equilibrium equation; hence,

$$\frac{\partial x_1}{\partial x_D} = \frac{\partial x_1}{\partial y_1} \cdot \frac{\partial y_1}{\partial x_D} = \frac{\partial e(y_1)}{\partial y_1} \cdot \frac{\partial y_1}{\partial x_D}. \tag{5}$$

y_2 is computed from x_1 using the operating relation; hence,

$$\frac{\partial y_2}{\partial x_D} = \frac{\partial y_2}{\partial x_1} \cdot \frac{\partial x_1}{\partial x_D} = \frac{\partial o(x_1)}{\partial x_1} \cdot \frac{\partial x_1}{\partial x_D}. \tag{6}$$

We continue this way, until we reach the bottom stage.

Differentiation of Eq. 3 gives Eq. 7, where all the terms are available:

$$\frac{\partial f}{\partial x_D} = -(V - L) + (x_D - x_N) \cdot \frac{\partial L}{\partial x_D} - (F - V + L) \cdot \frac{\partial x_N}{\partial x_D}. \tag{7}$$

Extension to higher-order derivatives is straightforward.

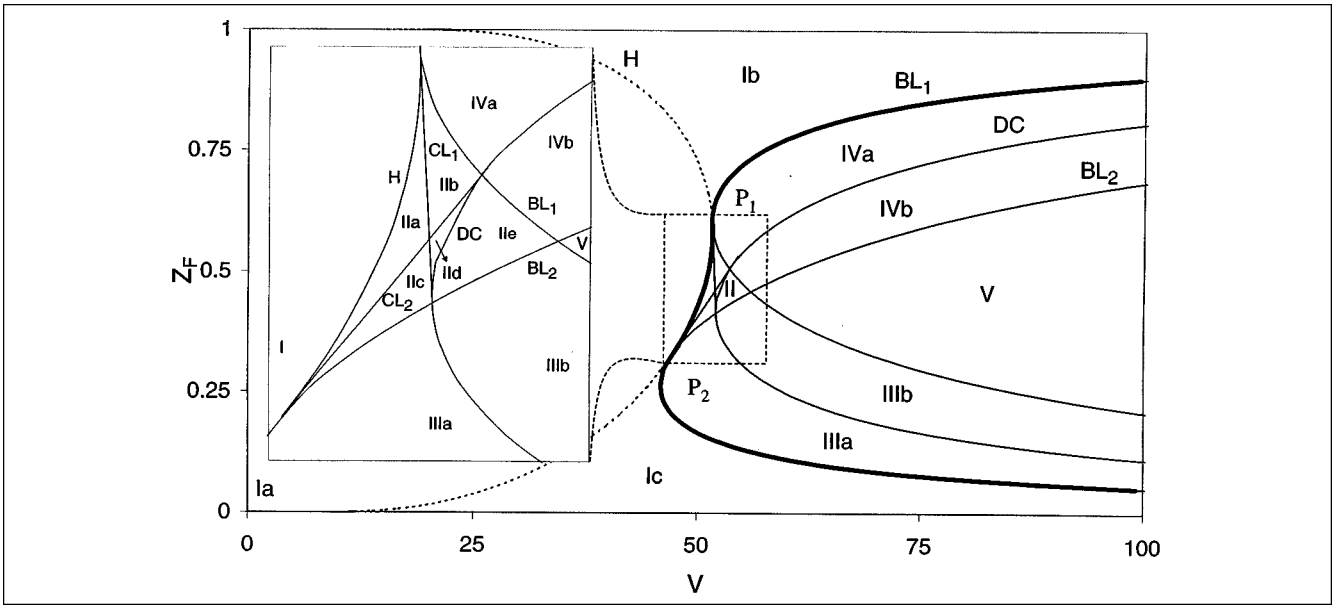

Figure 2. Typical phase diagram for ideal, constant molar overflow, binary distillation.

$\alpha = 1.1$; $M_1/M_2 = 0.9$; $N = 8$; $N_F = 4$. H—hysteresis; BL—boundary limit; DC—double cross; CL—cross-and-limit. Bold line represents the unicity-multiplicity boundary. Dashed line corresponds to occurrence of two unfeasible limit points. Different types of bifurcation diagrams existing in regions I–V are presented in Figure 3.

Results

Due to the large number of parameters involved, complete classification of the steady-state behavior is difficult. It is useful to divide the set of parameters into three groups:

1. Operation parameters: mass reflux (L_w), boilup (V), and feed composition (z_F)
2. Physical parameters: relative volatility (α), and molar weight ratio (M_1/M_2)
3. Design parameters: number of trays (N), and feed tray (N_F).

A codimension-2 variety determines the state variable and two parameters. One of them is the bifurcation parameter (L_w). We choose the boilup (V) as the second parameter. The location of a codimension-2 point (L_w, V) changes when a third parameter (z_F) is varied. This dependence can be traced and plotted in the ($V - z_F$) plane, for fixed values of

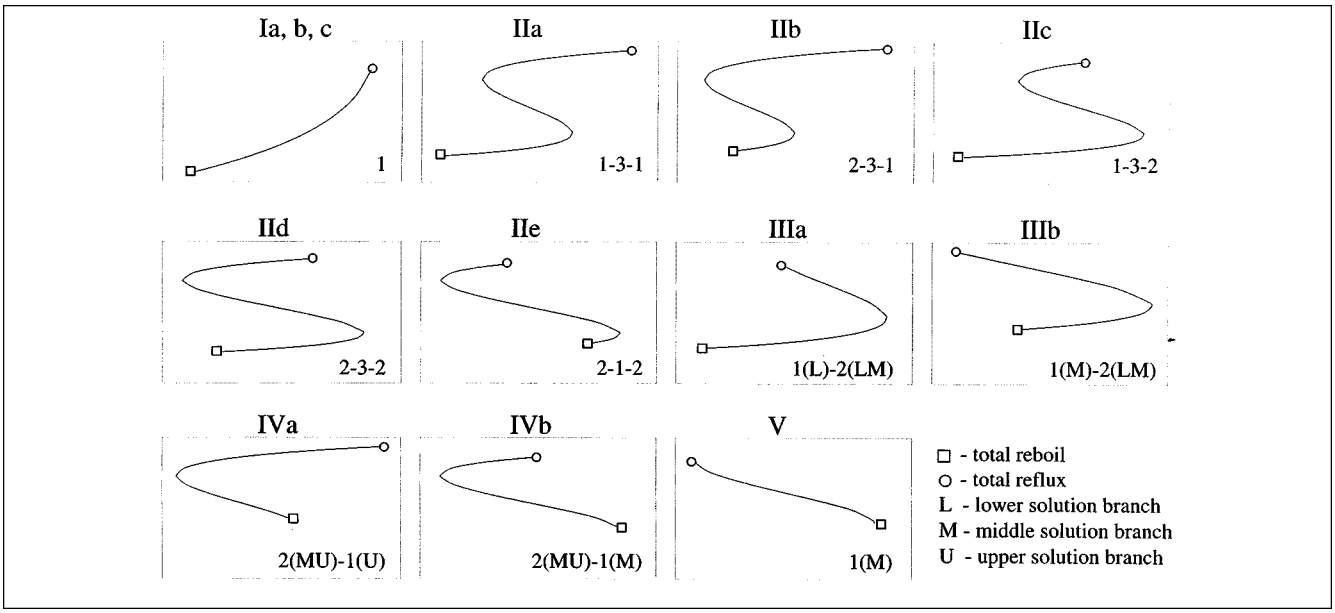

Figure 3. Distillate concentration vs. mass reflux bifurcation diagrams.

Diagrams I–V correspond to regions I–V in Figure 2.

the α, M_1/M_2, N, and N_F parameters. We used a continuation method based on local parametrization (Seydel and Hlavacek, 1987).

The codimension-2 varieties dividing the $(z_F - V)$ parameter space are presented in Figure 2. Figure 3 presents the bifurcation diagrams existing in different regions of Figure 2. In order to illustrate the steady-state behavior clearly, we chose extreme parameter values (a small column is used to separate a low relative volatility mixture). We discuss the influence of more realistic operation and physical parameters later.

The hysteresis variety is intersected tangentially by the two boundary-limit sets at codimension-3 singular points (P_1 and P_2). In region Ia, there is one steady state. Crossing the hysteresis variety to region Ib or Ic, two limit points appear. However, because they are located outside the feasibility region, state unicity is preserved. Crossing the BL_1 set from region Ib to region IV, one limit point passes the total reboil boundary and enters the feasibility region; hence, the multiplicity pattern in region IV is 2−1. Similarly, when the BL_2 set is crossed from region Ic to III, one limit point enters the feasibility region through the total reflux boundary; hence, the multiplicity pattern in region III is 1−2. Consequently, the multiplicity boundary (bold line in Figure 2) is given by a segment of BL_1 down to P_1, a segment of H between P_1 and P_2, and a segment of BL_2 beyond P_2. When going from region IV or III to region V, the BL_2 and BL_1 sets, respectively, are crossed. In each case, one limit point leaves the feasibility region (through the total reflux and the total reboil boundaries, respectively); hence, in region V, we again have state unicity.

Regions III and IV are further divided by the double-cross set into parts with different relative location of the total reboil and total reflux conditions. We denote by L, M, and U the lower, middle, and upper branches of the bifurcation diagram, respectively (regardless of their feasibility). Then, in regions IIIa and IIIb the multiplicity patterns are L-LM and M-LM, respectively. Similarly, the multiplicity patterns in regions IVa and IVb are MU-U and MU-M, respectively.

Two feasible limit points appear when the hysteresis variety is crossed from region Ia to region II. Region II is bounded by the H, BL_1, and BL_2 sets and divided by two cross-and-limit sets and the double-cross set. The 1-3-1 multiplicity patterns (IIa) becomes 2-3-1 (IIb), 1-3-2 (IIc), or 2-3-2 (IId), as CL_1 and CL_2 are crossed and the relative positions of one limit point and one feasibility boundary change. When the DC set is passed to region IIe, the relative location of feasibility boundaries changes; consequently, the multiplicity pattern becomes 2-1-2.

Figure 4 shows phase diagrams obtained for values of the α, M_1/M_2, N, and N_F parameters that are more realistic than those used in Figure 2. Although all the varieties and regions discussed previously are present, for clarity we displayed only the unicity−multiplicity boundary.

Diagram A shows the influence of relative volatility, for a mixture with small ratio of the molar weights. When α has practical values, the BL_1 variety moves very close to $z_F = 1$. The BL_2 variety is located at very small feed concentration and does not intersect the hysteresis for positive values of the boilup. Hence, the boundary between the unicity and multiplicity regions is the hysteresis variety. This conclusion is also valid for other practical situations. There is a region of small z_F that can lead to multiple steady states even at low boilup. For high z_F, practical boilup values can lead to multiple steady states if the components to be separated have high

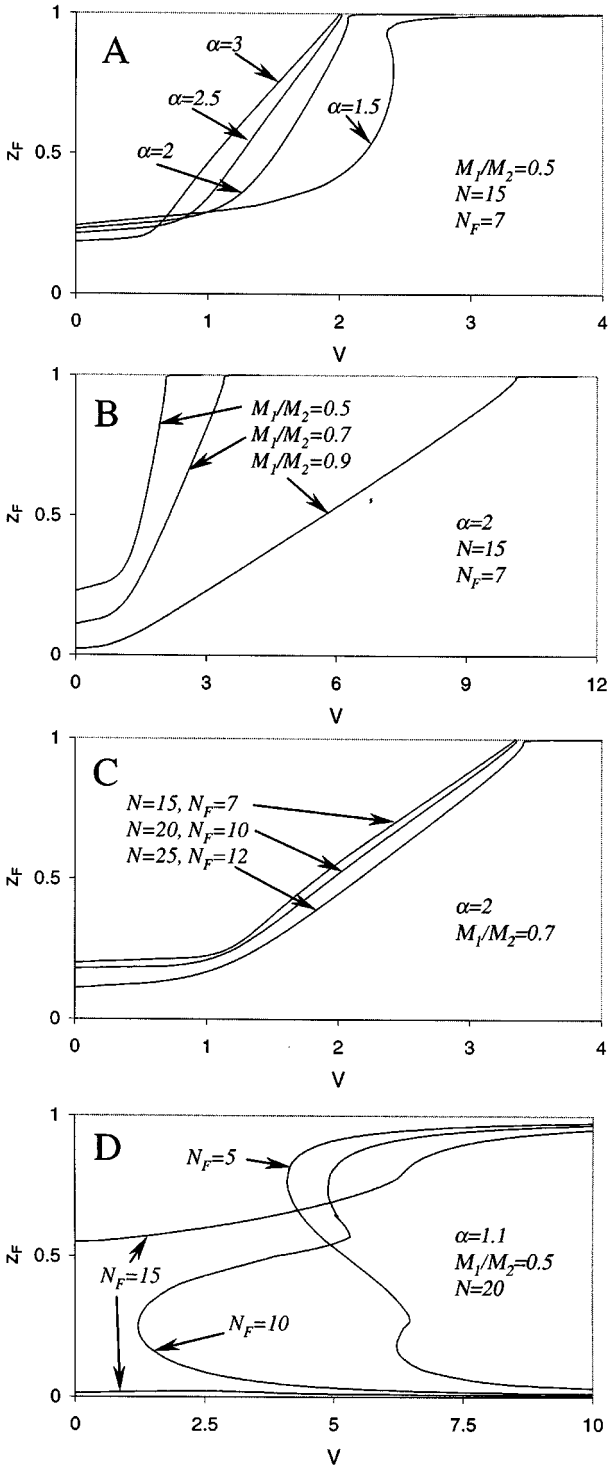

Figure 4. Influence of the model parameters on the extent and location of the multiplicity region.

Multiplicity region is larger for high relative volatility, low molar weight ratio, or feed close to the column bottom.

relative volatility. We also note that, at small boilup, increasing α slightly shifts the unicity region toward lower feed concentration.

Diagram B presents the influence of the molar-weight ratio, for a usual value of α. The size of the unicity region is larger when the components have similar molar weights. The effect of M_1/M_2 is more important at high feed concentration. When M_1/M_2 is close to the unity, multiplicity will probably occur for a low feed concentration or high internal flow rates. The number of trays has a small effect (Diagram C), while the location of the feed tray does not affect appreciable the multiplicity boundary.

The BL_1 and BL_2 varieties are located in Diagrams A–C for very high or low feed concentration, respectively. One exception is the low relative volatility case (Diagram D). In this situation, moving the feed location to the column bottom enlarges the multiplicity region.

In conclusion, computation of codimension-2 singular points and parameter sets was used to classify the steady-state behavior of ideal, constant molar overflow, binary distillation. Eleven different bifurcation diagrams are possible. Multiple steady states are likely to appear for practical situations when the relative volatility is large, the components have very different molar weights, or feed concentration is small.

Literature Cited

Baslakotaiah, V., and D. Luss, "Global Analysis of the Multiplicity Features of Multi-Reaction Lumped-Parameter Systems," *Chem. Eng. Sci.*, **39**, 865 (1984).

Golubitsky, M., and D. G. Schaeffer, *Singularities and Groups in Bifurcation Theory*, Springer-Verlag, New York (1985).

Jacobsen, E. W., and S. Skogestad, "Multiple Steady States in Ideal Two-Product Distillation," *AIChE J.*, **37**, 499 (1991).

Kienle, A., M. Groebel, and E. D. Gilles, "Multiple Steady States in Binary Distillation—Theoretical and Experimental Results," *Chem. Eng. Sci.*, **50**, 2691 (1995).

Seader, J. D., and E. J. Henley *Separation Process Principles*, Wiley, New York (1998).

Seydel, R., and V. Hlavacek, "Role of Continuation in Engineering Analysis," *Chem. Eng. Sci.*, **42**, 1281 (1987).

Manuscript received Mar. 29, 1999, and revision received June 29, 1999.